Rock Mech Rock Eng (2012) 45:289–309
DOI 10.1007/s00603-011-0199-5

ORIGINAL PAPER

A Top Pilot Tunnel Preconditioning Method for the Prevention of Extremely Intense Rockbursts in Deep Tunnels Excavated by TBMs

Chuanqing Zhang · Xiating Feng · Hui Zhou · Shili Qiu · Wenping Wu

Received: 21 June 2011 / Accepted: 26 October 2011 / Published online: 10 November 2011

Abstract The headrace tunnels at the Jinping II Hydropower Station cross the Jinping Mountain with a maximum overburden depth of 2,525 m, where 80% of the strata along the tunnels consist of marble. A number of extremely intense rockbursts occurred during the excavation of the auxiliary tunnels and the drainage tunnel. In particular, a tunnel boring machine (TBM) was destroyed by an extremely intense rockburst in a 7.2-m-diameter drainage tunnel. Two of the four subsequent 12.4-m-diameter headrace tunnels will be excavated with larger size TBMs, where a high risk of extremely intense rockbursts exists. Herein, a top pilot tunnel preconditioning method is proposed to minimize this risk, in which a drilling and blasting method is first recommended for the top pilot tunnel excavation and support, and then the TBM excavation of the main tunnel is conducted. In order to evaluate the mechanical effectiveness of this method, numerical simulation analyses using the failure approaching index, energy release rate, and excess shear stress indices are carried out. Its construction feasibility is discussed as well. Moreover, a microseismic monitoring technique is used in the experimental tunnel section for the real-time monitoring of the microseismic activities of the rock mass in TBM excavation and for assessing the effect of the top pilot tunnel excavation in reducing the risk of rockbursts. This method is applied to two tunnel sections prone to extremely intense rockbursts and leads to a reduction in the risk of rockbursts in TBM excavation.

Keywords TBM · Rockburst · Top pilot tunnel · FAI · ERR · ESS

C. Zhang (✉) · X. Feng · H. Zhou · S. Qiu · W. Wu
State Key Laboratory of Geomechanics and Geotechnical Engineering, Institute of Rock and Soil Mechanics, Chinese Academy of Sciences, Wuhan 430071, People's Republic of China
e-mail: cqzhang@whrsm.ac.cn

1 Introduction

With an intense impact of energy (Singh 1988; Tang 2000), rockbursts cause damages to rock mass by seismic events resulting from human excavation activities, indicated by the violent ejection of excavation-face rocks (Ortlepp 2001). A rockburst often causes heavy casualties and equipment losses, resulting in increased construction costs or even the abandonment of a project. Two concepts, a rockburst versus a seismic event, are easily confused. Li et al. (2007) clearly distinguished them by defining a rockburst as a particular seismic event caused by mining or tunnel excavation (i.e., a rockburst is the result of a seismic event, but not all seismic events lead to a rockburst).

There are many types of rockbursts, which can be classified based on the mechanism by which the rock mass is damaged (Board 1994; Brown 1984; Li et al. 2007; Ortlepp and Stacey 1994; Tang 2000). Ortlepp and Stacey (1994) thought that rockbursts in tunnel construction primarily includes strain-bursting, bulking, and face crush, whereas shear rupture and fault-slip types of rockbursts may occur in deep mining tunnels. Board (1994) suggested two basic mechanisms of rockbursts, the brittle failure of intact rock mass and the unstable slip along the primary weak plane, as reported in the literature. Therefore, rockbursts can be divided into strainbursts and fault-slip bursts. Tang (2000) proposed a rockburst that combines both strain and fault-slip. According to the statistical data, he showed

that the majority of rockbursts are classified as the strain type, even when the damage caused by strainbursts is relatively weak.

In fact, both types of rockbursts occur in deep civil engineering tunnels. Due to a smaller excavation scale and disturbed zone, the intensity of a rockburst in the civil field is, in general, weaker than that in the mining field. Fault-slip rockbursts mainly occur in mining tunnels in which the stress environment is largely affected by its surrounding mining working face (Ortlepp 2001). Due to the small influence zone, a large-scale fault-slip rarely occurs during the excavation of a civil engineering tunnel. Thus, a fault-slip rockburst in it generally refers to a small-scale slip on the structural plane, which is also called a structural-plane rockburst.

With the increase of very deep traffic tunnels and hydropower project tunnels in China, rockbursts often occur in tunnel construction. For example, a large number of rockbursts took place during the excavation of the Erlang Mountain roadway tunnel, the headrace tunnels at the Futang Hydropower Station, the Tianshengqiao II Hydropower Station, and the Ertan Hydropower Station, as well as in the auxiliary tunnels, drainage tunnels, and headrace tunnels at the Jinping II Hydropower Station, which caused heavy casualties and equipment damage.

Currently, most rockburst prevention methods applied to civil tunnels are introduced from mining engineering, which can be classified into three types: the optimization of the excavation scheme and pillar layout scheme, the surrounding rock mass support, and the preconditioning method. Salamon (1983) classified methods into strategic and tactical types. The strategic method is to minimize the risk of rockbursts by changing the project layout scheme and the excavation method, as well as optimizing the shapes, dimensions, and excavation sequences in the excavated section. Tactical methods are control measures applied to the inevitable risk of rockbursts in strategy. Moreover, Board (1994) proposed three types of rockburst prevention measures: optimization of the excavation method and sequence, the negative control method, and the positive control method. In addition to engineers' experience, the numerical analysis method based on the energy release rate (ERR) (Cook et al. 1966) and the excess shear stress (ESS) (Ryder 1988) is the main practical tool for the selection and optimization of a strategic scheme (Board 1994).

Under rockburst conditions, ground support is a major prevention measure. McCreath and Kaiser (1992) proposed to use the cable lacing support system. Based on a static loading test, Stacey et al. (1995) studied the energy absorption capacity of reinforced shotcrete. Hoek et al. (1997) proposed support control methods which aimed at spalling and damage to hard rock under high stress. Broch and Sørheim (1984) studied the supporting of a road tunnel subjected to heavy rockbursts.

Even with the most optimal design, the energy absorption capacity of support systems is only up to 50 kJ/m^2 (Canadian Rockburst Research Program, CRRP 1996). When the impact energy of an intense rockburst exceeds this maximum practical support limit, the support system alone will not be able to withstand the impact of rockburst. In such a situation, a preconditioning method, destress blasting or the fluid injection of faults (Board 1994), should be adopted. Destress blasting was first proposed and applied in the Witwatersrand gold mines in South Africa in 1950 (Roux et al. 1957), with subsequent success in mining engineering in South Africa and North America (Tang 2000). Destress blasting alters the mechanical properties and failure modes through the blast damage of the rock mass or primary structural planes, and reduces the risk of rockbursts by changing the stress distribution in the rock mass. The fluid injection of a fault avoids the risk by artificially controlling when a seismic event occurs (Board 1994).

Considering different excavation activities and application requirements for engineering structures, these methods in the mining fields cannot be directly applied to the civil fields. Necessary changes have to be made based on the actual situation in the field. Moreover, the application of these methods to tunnels is based on the excavation techniques, such as the D&B (drilling and blasting) method or the tunnel boring machine (TBM) method. For example, TBM equipment is bulky and cannot get around formations prone to rockbursts and, thus, destress blasting cannot be conducted in front of the cutter head.

Based on their statistical analysis of the relationship between rockburst position and tunnel face distance, Shan and Yan (2010) showed that the majority of rockbursts in tunnel projects occurred in a range of 2 diameters behind the tunnel face, while the initial supporting area of the TBM (L1 area) was located just within this range behind the shield. Because of the peak activity of rockbursts, the support construction is very difficult and dangerous in the L1 area. Thus, in most cases, this problem cannot be handled using the timely support measures. To a certain extent, mild or moderate rockburst events can be controlled by the timely use of shotcrete. However, intense rockbursts, especially rockburst events with an impact energy greater than 50 kJ/m^2, will have a devastating impact on TBMs.

The deep tunnel sections of the Jinping II Hydropower Station are prone to extremely intense rockbursts (Shan and Yan 2010; Wu et al. 2010). Of these tunnels, two headrace tunnels and a drainage tunnel are excavated by TBMs. In November 2008, the 7.2-m-diameter TBM in the drainage tunnel was destroyed by an extremely intense rockburst. Such serious rockbursts have not occurred in other tunnels in the world excavated by TBMs, such as the Steg lateral

adit of the Lötschberg base tunnels (Rojat et al. 2009) and the headrace tunnels at the Tianshengqiao II Hydropower Station in China (Li et al. 2007). In these tunnels, spalling was dominant, with no impact on the safety of equipment and personnel. In contrast, TBM excavation is more challenging in the deep tunnels at the Jinping II Hydropower Station.

To ensure the safety of TBMs in the two 12.4-m-diameter headrace tunnels, a combined excavation method is proposed to handle intense rockbursts during TBM excavation, consisting in the excavation and support of the top pilot tunnel by the D&B method with subsequent excavation using TBMs. It is based on a comprehensive analysis of the rockburst characteristics and different construction methods used in this project, as well as reference to destress blasting mechanisms.

A numerical analysis based on the failure approaching index (FAI) (Zhang et al. 2011a), ERR (Cook et al. 1966), and ESS (Ryder 1988) is conducted in order to study the mechanism of this method and the effect of reducing the strain-type and fault-slip type rockbursts. Combining theoretical analysis, construction feasibility discussion, and field tests, a comprehensive assessment of this method in reducing the risk of rockbursts is carried out. Finally, the successful application cases of this method in several tunnel sections prone to intense and extremely intense rockbursts are presented.

2 Analysis Method and Evaluation Indices

Numerical analyses are carried out to assess the effectiveness of the different schemes based on several indices. In addition, factors related to construction feasibility are also considered. For a better understanding of the process and results, the numerical analysis tools and evaluation indices are presented first in this section. Then, the different issues on construction feasibility will be discussed in the analysis section.

2.1 Tools and Conditions of Numerical Analysis

The stress and strain analyses are conducted using a simulation of the linear and non-linear mechanical behavior of the surrounding rock mass. In order to precisely simulate the post-peak mechanical behavior of the rock mass induced by excavation so as to reasonably evaluate the different pilot tunnel schemes, the FLAC^{3D} version 3.1 computer code, equipped with a strain hardening or softening model, is used as a numerical tool, and the three-dimensional models are built and the FISH codes for the control of excavation are programmed. In FLAC^{3D}, the minimum, intermediate, and maximum principal stress components are expressed as σ_1, σ_2, and σ_3, respectively, i.e., $\sigma_1 < \sigma_2 < \sigma_3$. Unless specifically indicated, tension and extension are considered to be positive and compression to be negative. These same conventions are adopted throughout this paper.

A linear elastic constitutive model is adopted for the analysis based on the ERR and the ESS, and the cohesion weakening and frictional strengthening (CWFS) model (Hajiabdolmajid et al. 2002) is used for the analysis based on the FAI. The choice of the models is not optional, but is determined by evaluation theories. The mechanical parameters of T_{2b} marble are listed in Table 1, all of which were obtained by a back-analysis based on field monitoring data.

To compare the schemes, typical tunnel sections at depths of 1,900 and 2,500 m prone to intense or extremely intense rockbursts are selected. The in situ stress components are listed in Table 2, and the coordinate system used is shown in the solid line frame in Fig. 1. The y-axis is horizontal and directed to the west end of the tunnels along the tunnel axis, and the x-axis is orthogonal to the y-axis, in the tunnel cross-section. The z-axis is upward in the vertical direction.

2.2 Evaluation Index: FAI

To evaluate the stress concentrations and the degree of damage of the surrounding rock mass, the FAI was presented by Zhang et al. (2011a) as follows:

$$\mathrm{FAI} = \begin{cases} \omega & 0 \le \omega < 1 \\ 1 + \mathrm{FD} & \omega = 1, \mathrm{FD} \ge 0 \end{cases} \quad (1)$$

where ω is the phase complementary parameter of the yield approach index (YAI) that is defined to evaluate stress concentrations in the principal stress space and FD (failure degree) is the index for evaluating the degree of damage accumulation during deformation and fracturing of the rock mass.

Here, the FAI is obtained by using the CWFS model in order to understand the mechanism of rock mass rupture

Table 1 Mechanical parameters for Jinping II T_{2b} marble

Parameters	Values
Elastic modulus	18.9 GPa
Poisson's ratio	0.23
Initial cohesion	15.6 MPa
Residual cohesion	7.4 MPa
Initial internal friction angle	25.8°
Residual internal friction angle	39.0°
Plastic strain limit for cohesion	4.5%
Plastic strain limit for friction angle	9.0%
Dilation angle	10°

Table 2 The in situ stress components of the sections with depths of 1,900 and 2,500 m

Depth (m)	σ_x (MPa)	σ_y (MPa)	σ_z (MPa)	τ_{xy} (MPa)	τ_{yz} (MPa)	τ_{xz} (MPa)
1,900	−48.54	−49.97	−51.46	−0.35	−3.23	5.82
2,500	−51.20	−55.67	−66.48	−1.10	−6.11	4.58

and stress transformation, based on the top pilot and central pilot tunnel excavation schemes. The difference in the FAI distribution calculated is used as a basis for comparing the results obtained.

2.3 Evaluation Index: ERR

Since it was introduced by Cook et al. (1966) in 1960s, the energy release rate (ERR) has become the most widely used index to evaluate how prone the intact rock mass is to strainburst (Board 1994), and has been applied to the design of working face form and pillar layout schemes (Tang 2000). The relationship between the ERR and rockburst has been widely used as a tool to predict rockbursts developed during gold excavation in South Africa.

The energy conversion principle in the process of underground mining was studied by Salamon (1984). In his study, the released energy induced by a change in the system state is $U_m + W_k$, where U_m is the sum of the strain energy stored in the rock volume to be mined, V_m, and W_k is the kinetic energy induced by the instantaneous removal of all of the rock in V_m. U_m can be released by smashing the mined rock mass. Therefore, in fact, W_k is the excess energy that should be transferred to kinetic energy or consumed in the surrounding rock mass by fracturing. It can be obtained from the product of the traction on the excavation surface of the next step before excavation by the closure of this surface after excavation. This portion of the energy was also taken to be the released energy, W_r, by Brady and Brown (2006), in which U_m is not included. In every excavation step, the volume rate of energy released, dW_r/dV_m, is an index of the specific energy available for the local crushing of rock around the excavation boundary.

In this study, the different shapes and sizes of pilot tunnels will alter the magnitude of released energy and the pattern of energy dissipation in the surrounding rock mass of the main tunnel excavated by TBMs. The risk of rockbursts will be reduced due to the pilot tunnel effect, which should be reflected in the evaluation variable. As an important variable for the optimization of face shapes (Board 1994), the ERR is useful in this study for assessing how prone rockbursts are in the different pilot tunnel schemes, although one limitation is the inability to reflect the inelastic behavior of the rock mass. Therefore, it is not the only variable for the evaluation of pilot tunnel schemes. Even so, the results from the analyses based on the ERR are very important for comparing and choosing the pilot tunnel schemes.

2.4 Evaluation Index: ESS

As an energy method based on continuum mechanics, the ERR can only be used to assess how prone an intact rock

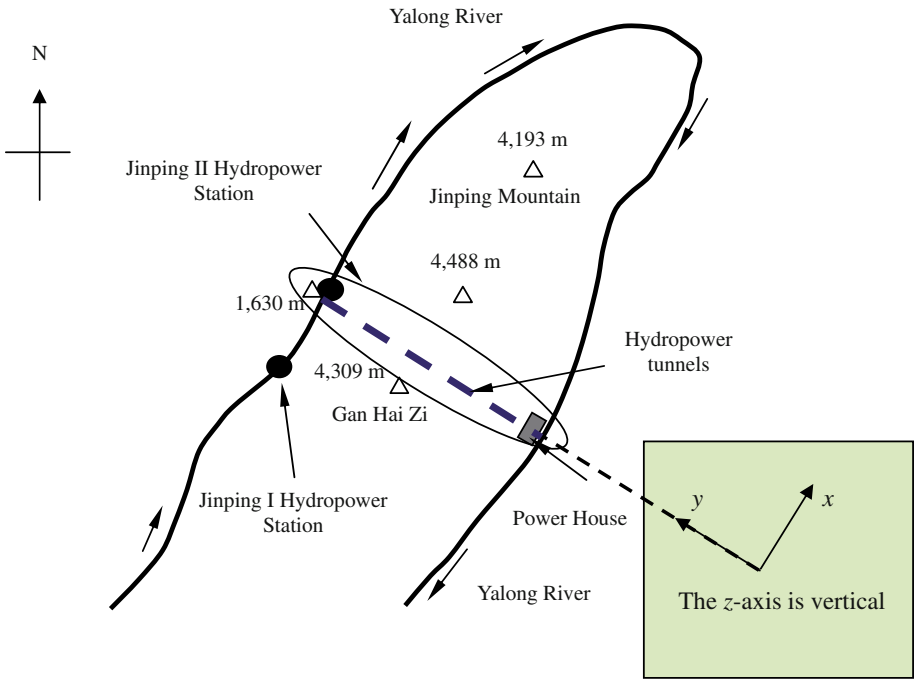

Fig. 1 The location of the Jinping II Hydropower Station

mass is to strainburst, but fault-slip rockbursts caused by a slip along the primary structural plane in the rock mass due to high stress are ignored (Board 1994). Based on the understanding of the fault-slip rockburst mechanism, Ryder (1988) proposed the concept of excess shear stress (ESS), which was expressed as the difference between the shear stress on the discontinuity before slip and its dynamic shear strength:

$$\mathrm{ESS} = \tau_e = |\tau| - \mu_d \sigma_n \tag{2}$$

where τ is the shear stress on the discontinuity before the slip, μ_d is the dynamic friction coefficient of discontinuity, and σ_n is the normal stress.

A slip of a geological discontinuity is activated due to the shear stress of a certain position exceeding the static shear strength τ_s, i.e., $\tau \geq \tau_s$. The latter is expressed as follows:

$$\tau_s = c + \mu_s \sigma_n \tag{3}$$

where τ_s is the static shear strength before slip, c is the cohesion, controlled by fillings, convex occlusion, or cohesive degree, and μ_s is the static friction coefficient of the discontinuity.

The initiation of shear failure at a certain position on the discontinuity will induce a chain reaction of shear failure of the other positions on the discontinuity, ultimately leading to a dynamic slip (Ryder 1988). Therefore, the relationship between shear stress and static shear strength of the discontinuity is crucial in order to assess whether a fault-slip rockburst occurs or not.

The ESS is introduced in this study for the interaction between the structural plane and the tunnel. The numerical analysis strategies proposed by Board (1994) are utilized. The stress distribution is based on the calculation of continuum elasticity. Then, shear stress is calculated given the strikes and dip angles of various discontinuities. Combined with the static shear strength of the discontinuity, an assessment is conducted on whether a shear slip event occurs or not. The 3D calculation methods for normal and shear stresses as provided by Goodman (1980) are used.

3 Presentation of the Problem

3.1 Project Overview

Located in Sichuan Province, China, the Jinping II Hydropower Station has a power capacity of 4,800 MW. Using a 310-m natural drop along the 150-km-long river bend in Yalong River around Jinping Mountain, this station is designed to cut the river bend, as shown in Fig. 1. With a rated head of 288 m, the Jinping II Hydropower Station has the highest water head and the largest power capacity among the cascade-developed power stations in the Yalong River Basin (Wu et al. 2010). The key project is the design and construction of four 16.7-km-long headrace tunnels, as shown in Fig. 2. They cross the Jinping Mountain with an orientation of N 58° W, where the maximum overburden depth is 2,525 m, and more than 75% of the tunnel sections have an overburden depth greater than 1,700 m. This is considered to be one of the deepest hydraulic tunnels in the world.

The design layout scheme of the headrace tunnels is shown in Fig. 2, where the headrace tunnels #1 and #3 have a 12.4-m-diameter circular section and are excavated using TBMs, and the headrace tunnels #2 and #4 have a 13-m-diameter circular section and are excavated using the D&B method. The centerline spacing among the four headrace tunnels is 60 m. In addition to the four headrace tunnels, another two auxiliary tunnels, i.e., #A and #B, have been excavated for transportation and exploration purposes in advance. A drainage tunnel, located between the auxiliary tunnel #B and the headrace tunnel #4, is excavated by a 7.2-m-diameter TBM. The centerline spacing between the two auxiliary tunnels and the drainage tunnel is 35 m, and that between the drainage tunnel and the headrace tunnel #4 is 45 m.

The geological cross-section of the headrace tunnels is shown in Fig. 3. Eighty percent of the tunnel rocks consist of marble, and the west end of the tunnel crosses a small number of chlorite schist, green sandstone, and sandy slate. The marble is characterized by a brittle behavior and high strength (with a uniaxial compressive strength of about 100 MPa and a tensile strength of 3–6 MPa). So, under great depths below the surface, intense rockbursts are, indeed, anticipated.

Based on field measurements and back-analysis results, the in situ stress conditions for the tunnel sections with an overburden depth greater than 1,900 m can be defined as follows:

- The angle between the minimum principal stress, σ_1, and the vertical direction is about 15°–35°, the intermediate principal stress, σ_2, is approximately horizontal along the tunnel axis, and the maximum principal stress, σ_3, is also approximately horizontal and perpendicular to the tunnel axis;
- The stress ratio σ_3/σ_1 is equal to 0.8–0.9;
- Local stress is concentrated in a synclinal core and anticline wing. In addition, due to the presence of a fault, the magnitude and direction of the adjacent in situ stress will change.

The in situ stress directions in the tunnel cross-section are shown in Fig. 4.

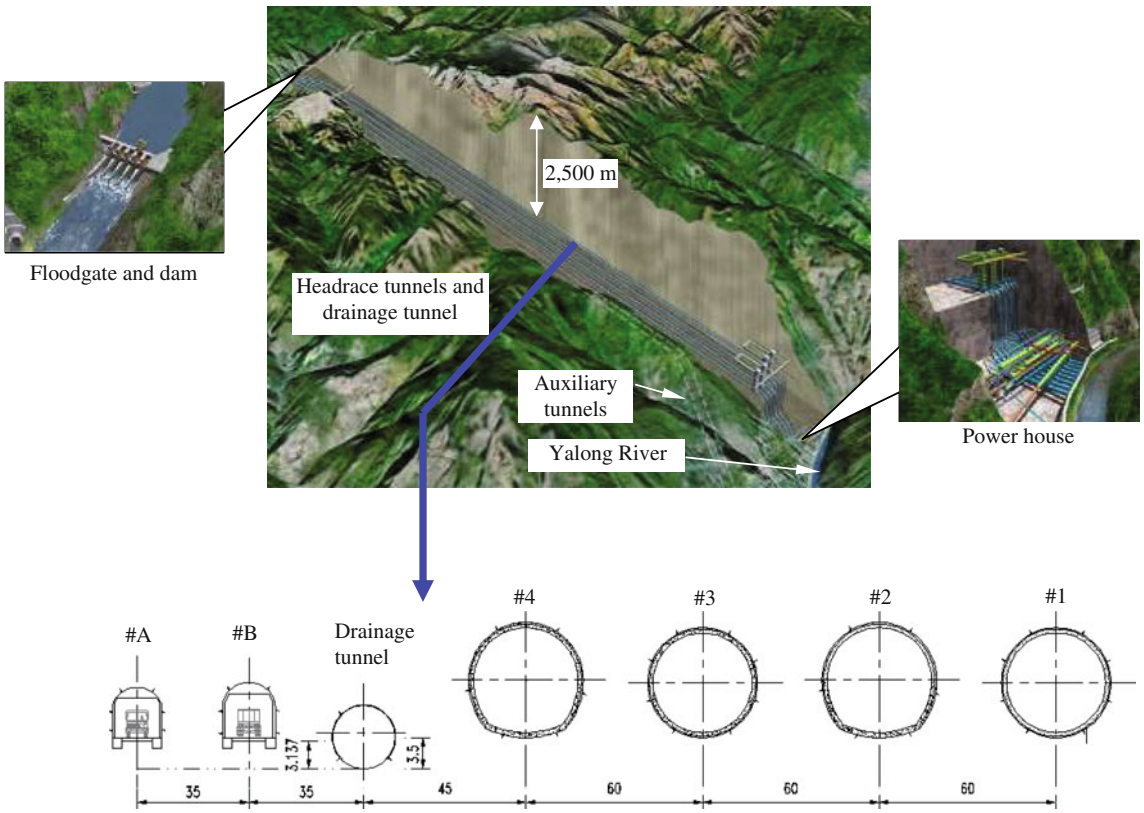

Fig. 2 The layout of the tunnels at the Jinping II Hydropower Station (m)

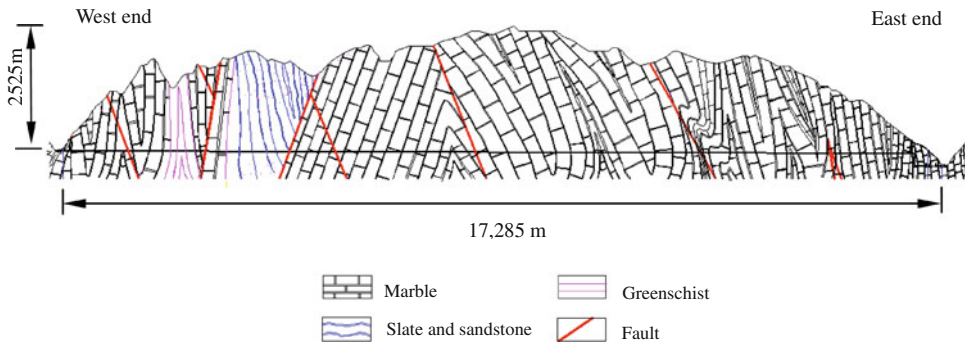

Fig. 3 The geological cross-section along the headrace tunnels at the Jinping II Hydropower Station

3.2 Characteristics of Rockbursts in the Auxiliary Tunnels

Due to the brittle behavior of marble and the high in situ stress, more than 270 rockbursts occurred during the excavation of the auxiliary tunnels, causing frequent casualties and equipment damages. For an evaluation of rockburst intensity, four grades were proposed in the tunnels at the Jinping II Hydropower Station by Shan and Yan (2010), as follows: light class (Grade I), middle class (Grade II), intense class (Grade III), and extremely intense class (Grade IV). Figure 5 shows the extremely intense rockburst on the north sidewall of the auxiliary tunnel #B at a depth of 2,300 m. Due to the severe impact, grid arch frames, steel fiber shotcrete, and fractured rock mass were ejected to the opposite sidewall, the surface support system was damaged, and almost all of the rock bolts were pulled out. Under the huge impact, a steel plate was detached from the bolts. Due to the very high compressive stresses, the rock mass was seriously fractured.

Statistics show that the cumulative lengths of the rockburst sections in the auxiliary tunnels #A and #B are 3,259.5 and 2,957.2 m, respectively, accounting for 18.48 and 16.29% of the total length of the tunnels, respectively. The extremely intense rockbursts occur along 301.5- and 241-m tunnel lengths, respectively, accounting for 1.73 and 1.39% of the total length of the tunnels (Shan and Yan 2010).

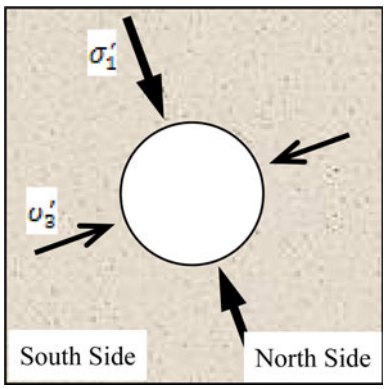

Fig. 4 Schematic diagram of the directions of the in situ stress in the tunnel section at a depth greater than 1,900 m

Fig. 5 The extremely intense rockburst at BK9+516-538 in the auxiliary tunnel #B

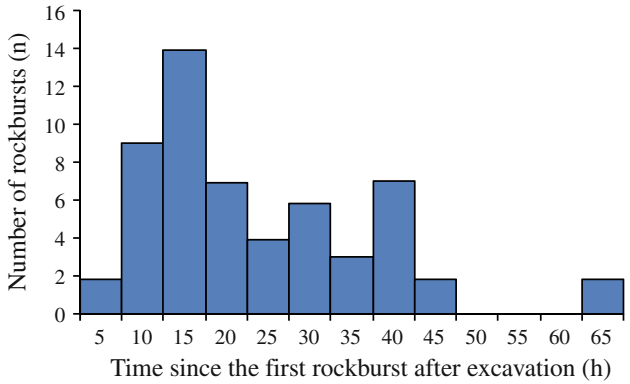

Fig. 6 The relationship between the number of rockbursts and the time since the first rockburst after excavation (Shan and Yan 2010)

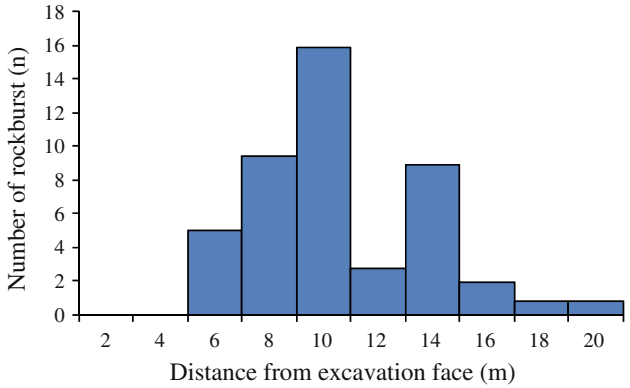

Fig. 7 The relationship between the number of rockbursts and their distance from the working face (Shan and Yan 2010)

Because the other tunnels run parallel to the auxiliary tunnels, the same in situ stress and similar geological conditions along these tunnels mean that there is at least an equivalent risk of rockbursts. An enormous challenge arises during the subsequent TBM excavation of the drainage tunnel and the headrace tunnels #1 and #3. Therefore, a full understanding of the characteristics and the temporal-spatial development of rockbursts in the auxiliary tunnels is of the utmost importance as a guide to rockburst prevention.

The rockburst activities in the auxiliary tunnels included an active phase and a persistent phase. In the active phase, rockbursts generally occurred within a few hours after excavation, i.e., the most active one within 5–20 h. Most rockbursts occurred within this period, as shown in Fig. 6. Due to fracture development and the continuous adjustment of stresses in the surrounding rock mass, a number of rockbursts still occurred in the same position over the following several months. Rockburst activities were characterized by persistence in time, but with a significant reduction in the occurrence frequency. Ninety percent of rockbursts occurred within 16 days after excavation, 62% within 8 days, and 22% within 1 day. Figure 5 shows the extremely intense rockburst that occurred 1 week after the completion of supports.

Spatially, rockbursts mainly occurred about 6–12 m away from the tunnel face, as shown in Fig. 7.

3.3 Limitations of TBM Excavation in Tunnel Sections Prone to Rockbursts

The drainage tunnel and the headrace tunnels #1 and #3 are excavated by TBMs. The US-made Robbins hard rock boring machines are used in the drainage tunnel and the headrace tunnel #1, respectively. The total length of the machine in the headrace tunnel #1 is 210 m. A German-made Herrenknecht hard rock boring machine is used in the headrace tunnel #3, which has a total length of 172.5 m.

Figure 8 shows the functional zoning chart for TBMs. The shield extends 6.5 m behind the cutter head. To ensure the stability of the cutter head, the roof shield usually props up the top arch with a specific support on the surrounding rock mass during excavation. L1 refers to the area which extends 3.5 m behind the shield, i.e., the initial support

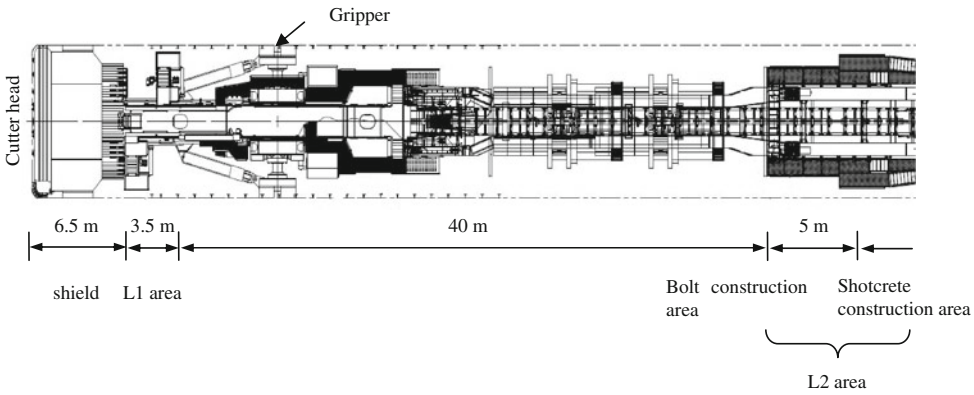

Fig. 8 The functional zoning chart for the tunnel boring machine (TBM) equipment

operations area where shotcrete, steel arches, and rock bolts installation is conducted. Therefore, personnel and equipment are mostly concentrated in this area. L2 refers to the area 40 m behind the L1 area, which is the supplementary support operations area.

The TBM method has the advantages of high mechanization and rapid excavation in sections with good stability (the maximum monthly advance reached 683 m in the marble tunnel section of the headrace tunnel #3 at a depth of less than 1,500 m). However, in the sections with serious brittle failure, the TBM equipment has many limitations.

For example, in theory, timely support can be carried out immediately after the shield passes in the L1 area. However, in the high-stress conditions, it is very difficult because of collapses, rockbursts, and other damages in this area with the advance of the working face and the shield, as shown in Fig. 9a. Figure 7 shows that the peak in the number of rockbursts occurred 6–12 m behind the tunnel face just in the L1 area where rockburst is a large threat to both personnel and equipment.

Blasting with the D&B method is known to cause an uneven excavation surface with local stress concentrations, easily inducing rockbursts. In contrast, TBM excavation is considered to be able to avoid this problem. In fact, blasting with the D&B method often causes damage to the rock mass, resulting in the formation of a protected area and the transfer of high stress to the deep surrounding rock mass. The low disturbance of TBM results in the high-stress concentration in a superficial

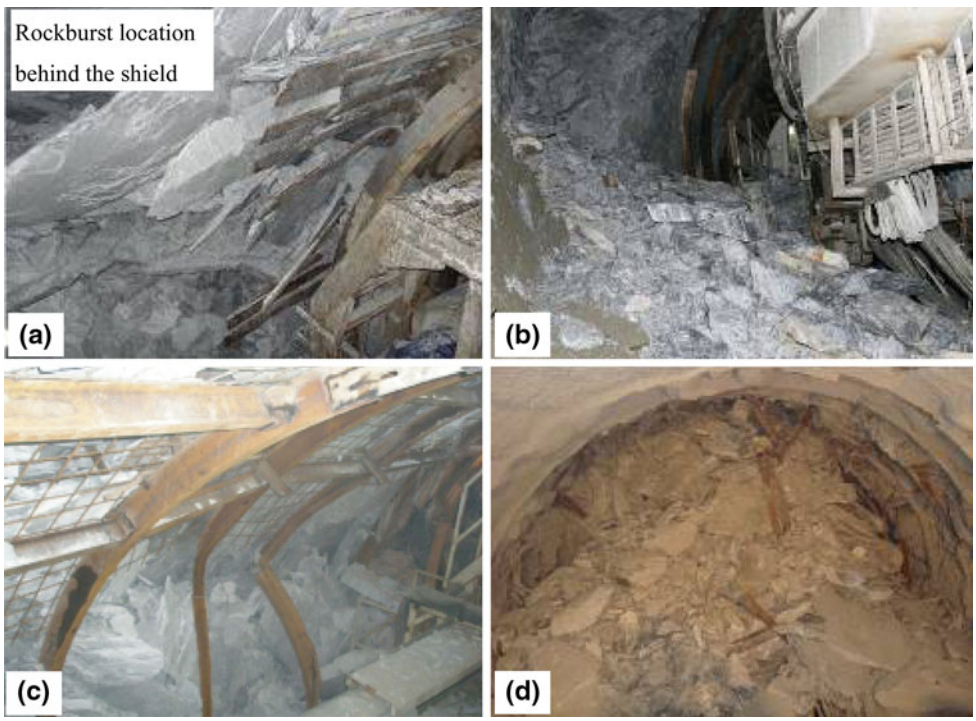

Fig. 9 The rockburst events in the construction of the drainage tunnel: **a** the moderate rockburst behind the finger-shaped shield on March 7, 2009; **b** the intensive rockburst on the south sidewall on August 17, 2008; **c** the intensive rockburst on the north sidewall on September 12, 2008; **d** the extremely intense rockburst on November 28, 2009

zone surrounding the rock mass, and then causing more serious damage.

In addition, the following limitations exist objectively as well:

(a) TBM equipment consists of a huge system and a narrow operating space with no flexibility. Therefore, other large machines cannot enter the emergency area for operations. In the case of a rockburst, collapse, or other incident, the cleaning of waste work must be done manually, which is time-consuming and often results in several weeks or months of downtime.
(b) Because the TBM equipment is a complete system, a shutdown for maintenance is necessary in case of any damage to any part of the system.
(c) No retreat is permitted. Thus, there is no flexibility to avoid the peak of a rockburst as with the D&B method.
(d) TBM equipment is relatively poor in resisting the impact of a rockburst.
(e) Destress blasting and other preconditioning methods cannot be applied.

On August 17, 2008, an intense rockburst occurred on the south sidewall of the drainage tunnel, causing TBM shutdown for 8 days, as shown in Fig. 9b. On September 12, 2008, a rockburst occurred on the north sidewall of the drainage tunnel with a 0.5–2-m-deep failure zone. The impact led to steel arches being broken, with a downtime of 4 days, as shown in Fig. 9c. On November 28, 2009, an extremely intense rockburst occurred in the drainage tunnel, and the TBM equipment was buried along a 28-m-long section. The main beam of the TBM was broken, the complete set of equipment was abandoned, and several casualties and major economic losses occurred, as shown in Fig. 9d.

Rockbursts during the excavation of the drainage tunnel show that the TBM equipment provides no solutions for preventing a rockburst. A large number of rockbursts in the excavation of the drainage tunnels and the auxiliary tunnels also imply that rockbursts are inevitable during the TBM excavation of the headrace tunnels #1 and #3. On-site engineers have to find out how to minimize the intensity and frequency of rockbursts, and avoid the highly destructive impact on equipment from extremely intense rockbursts.

4 Proposition and Demonstration of the Treatment Method

Important insights have been obtained by understanding some phenomena revealed during the excavation of the headrace tunnels #2 and #4.

Both the headrace tunnels have a 13-m diameter and upper and lower bench heights of 8.5 and 4.5 m, respectively, as shown in Fig. 10. All of the rockbursts in both tunnels occurred in the process of the upper bench excavation. These were less destructive because a flexible construction organization with personnel and equipment had been adopted to avoid the peak period of rockburst activities.

In addition, rockbursts never occurred during the lower bench excavation. The reasons for this are as follows:

(a) For the rock masses surrounding the upper bench, the high-stress concentrations have transferred to the interior and will not be disturbed significantly by the lower bench excavation.
(b) The supports consisting of rock bolts and shotcrete around the upper bench can provide security during the lower bench excavation.
(c) The energy cumulating in the lower bench rock masses has been consumed or released by their ruptures and deformation during the upper bench excavation.

Figure 11 shows the platy rock mass exposed in the lower bench excavation. Due to vertical sudden unloading and horizontal compression after the upper bench excavation, horizontal platy fractures occurred to the lower bench rock mass, resulting in a great reduction of its storage energy.

These phenomena indicate that a top pilot tunnel similar to the upper bench previously excavated with the D&B method may greatly reduce the intensity and frequency of rockbursts during TBM excavation. On this basis, the top pilot tunnel method is proposed and demonstrated. Its contents, demonstration process, and results will be described in this section.

4.1 Proposition of the Top Pilot Tunnel Method

After the extremely intense rockburst in the drainage tunnel on November 28, 2009, the top pilot tunnel scheme shown

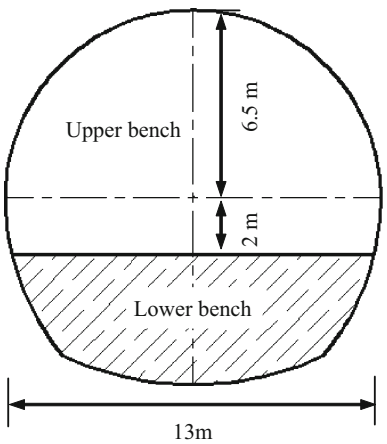

Fig. 10 The excavation scheme for the headrace tunnels #2 and #4

Fig. 11 The platy rock mass on the lower bench of the headrace tunnel #2

in Fig. 12a was proposed. Because it is excavated in the upper part of the tunnel cross-section, this tunnel is called the top pilot tunnel, to distinguish it from the other pilot tunnels used in rock engineering. For convenience, the final cross-section of the tunnel is called the main tunnel, and the part of the rock mass excavated by the TBM is called the rock mass of the main tunnel in all of the excavation schemes with or without the pilot tunnel. Note that the excavation of the main tunnel is different from the full-face excavation mentioned in the following.

The design principles of this scheme are as follows:

(a) To reduce the risk of rockbursts during the top pilot tunnel excavation as much as possible;
(b) To minimize the risk of rockbursts during TBM excavation;
(c) To use the TBM equipment to its maximum capacity.

The scheme includes the following key features:

(a) To estimate how prone the tunnel sections are to intense or extremely intense rockbursts;
(b) To excavate a bypass tunnel with the D&B method, or a transverse branch tunnel between neighboring main tunnels, prior to excavation of the pilot tunnel;
(c) To excavate the top pilot tunnel by the D&B method and carry out initial support;
(d) To excavate the remaining portion by the TBM method and complete the initial support.

Note that the top arch in the top pilot tunnel should be over-excavated to ensure that the outer heads of the rock bolts at the top arch are completely covered by shotcrete and to avoid damage to the TBM roof shield, as shown in Fig. 12a. The support measures of the top arch should be designed based on the tunnel section characterized by intense or extremely intense rockbursts.

Because the top pilot tunnel is excavated by the D&B method, geological radar or borehole drilling can be applied in order to understand the geological conditions in the heading and assess the propensity for rockbursts. Thereby, the destress blasting method and support measures can be applied during the pilot tunnel excavation. Meanwhile, the geological structures of the main tunnel can be sufficiently surveyed so as to assess the rockburst proneness during TBM excavation. If necessary, destress blasting can also be adopted as a supplementary measure to reduce the risk of rockbursts during the main tunnel excavation.

In the initial phase of the scheme demonstration, the central pilot tunnel option is also proposed, as shown in

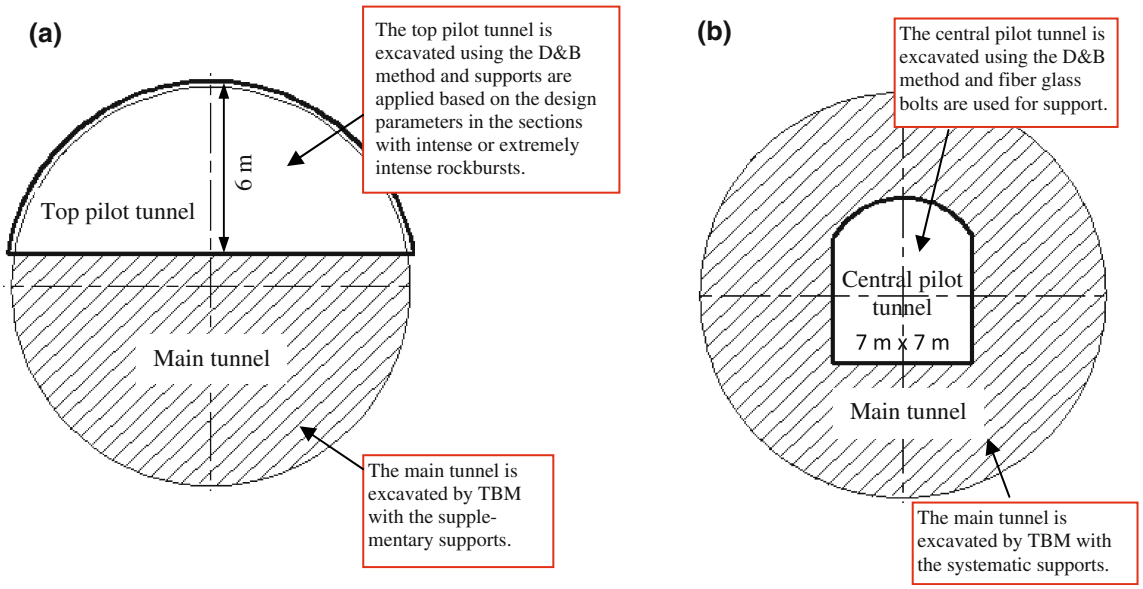

Fig. 12 Schemes for: **a** the top pilot tunnel (no sidewalls) and **b** the central pilot tunnel

Fig. 12b, but a dispute arises as to which scheme is better. In order to provide a sufficient basis for decision-making, a comparative analysis is conducted from both theoretical and construction points of view.

The mechanism of rockburst prevention using the pilot tunnel option is similar to that of destress blasting, i.e., the pilot tunnel excavation induces fractures in the surrounding rock mass and weakens its mechanical properties, so that the failure mode will be transformed from brittle to ductile. Meanwhile, the high stresses around the main tunnel will transfer to the internal rock mass.

Figure 13 shows the FAI distribution in the surrounding rock mass after excavation of the top pilot and main tunnels. The dashed line is the FAI contour after excavation of the top pilot tunnel and the solid line is that after excavation of the main tunnel. The region with FAI > 1 indicates that fractures occur to the rock mass exposed in the top pilot tunnel. And the contour line FAI = 1 far away from the tunnel surface indicates that high deviatoric stress concentrations have transferred to the internal rock mass, as shown in Fig. 15a. These indicate that the weakening of the surrounding rock mass and the redistribution of stress in the main tunnel have been achieved.

After excavation of the main tunnel, no significant change occurs to the FAI distribution formed during excavation of the top pilot tunnel, while only the FAI distribution in the surrounding rock mass exposed in the lower half of the main tunnel varies significantly. This indicates that the excavation of the main tunnel has little influence on the rock mass previously exposed, so that the risk of rockbursts can be greatly reduced.

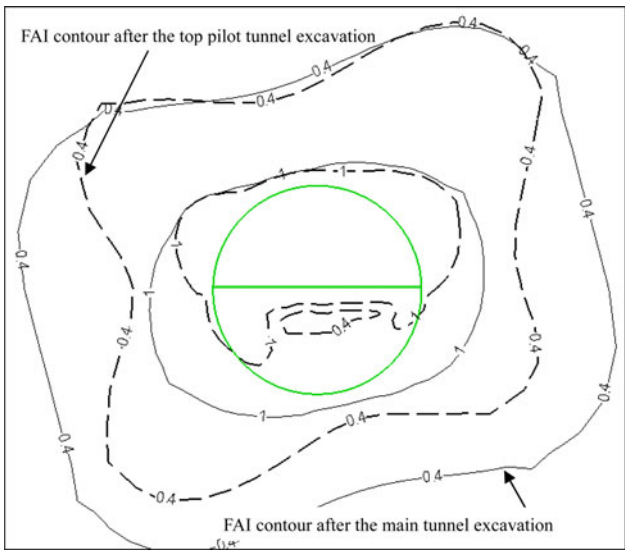

Fig. 13 The failure approaching index (FAI) distribution in the surrounding rock mass after excavation of the top pilot and main tunnels

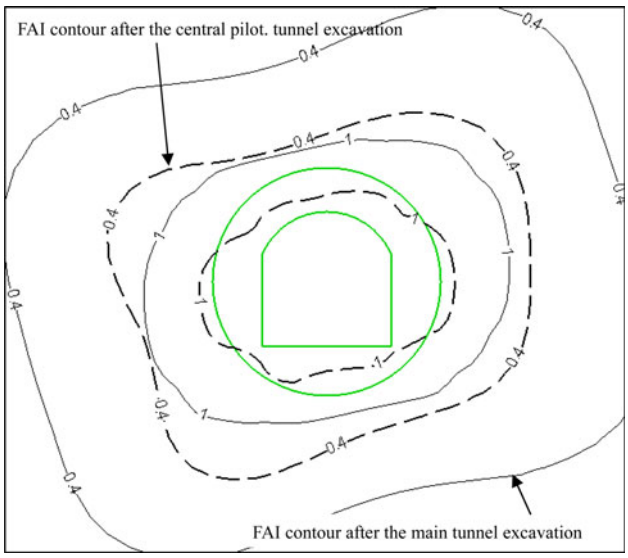

Fig. 14 The FAI distribution in the surrounding rock mass after the excavation of the central pilot and the main tunnels

Figure 14 shows that fractures (FAI > 1) occur to the surrounding rock mass after the central pilot tunnel excavation. But most of these fractured rock masses will be excavated by the TBM. The contour line FAI = 1 approaches the profile of the main tunnel. This indicates that the central pilot tunnel excavation cannot weaken the surrounding rock mass, or even cause the deviatoric stress and strain energy concentrations around the main tunnel, as shown in Fig. 15b. As a result, the intensity and frequency of rockbursts may increase during the main tunnel excavation with respect to the full-face TBM excavation or the pilot tunnel excavation.

This problem has been confirmed using the engineering case studies. The diversion tunnel on the left bank of the Ertan Hydrocarbon Station was excavated by the D&B method and had a 17.5-m × 23.5-m (width × height) cross-section. To prevent rockbursts, the central pilot tunnel was excavated with a 7-m × 8-m (width × height) cross-section. During the main tunnel excavation with the central pilot tunnel excavated in advance, the intensity and frequency of rockbursts were significantly enhanced compared to those in the pilot tunnel. Particularly, sudden rockbursts as a sector ejection occurred rarely in the pilot tunnel, while they were very common in the main tunnel excavation (Shi 1995).

In addition, because steel will damage the cutter head of the TBM, steel supports are not permitted in the cutting range. Moreover, steel bolts, steel plates, steel arches, steel mesh, etc. are prohibited for use in the central pilot tunnel support. Thus, only shotcrete and fiber glass bolts can be used, although the latter has poor shear properties. The support strength of the central pilot tunnel is so weak that

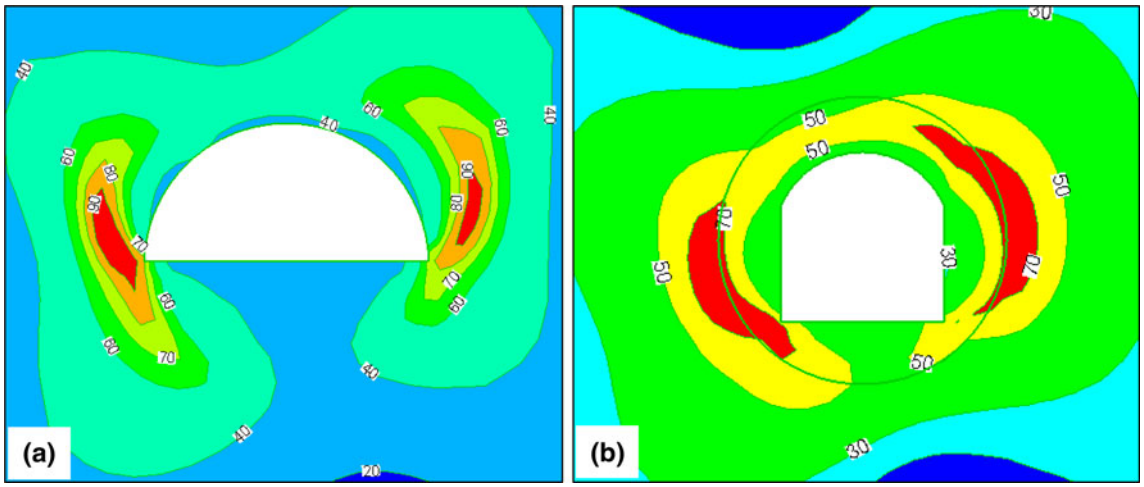

Fig. 15 The distribution of the deviatoric stress in the surrounding rock mass after the pilot tunnel excavation: **a** the top pilot tunnel and **b** the central pilot tunnel

it is difficult to provide security for the workers and equipment during the central pilot and main tunnel excavations.

As indicated by the results for the FAI and stress distribution, the top pilot tunnel method is more effective than the central pilot approach in reducing the risk of rockbursts in the main tunnel.

Nevertheless, the top pilot tunnel (as shown in Fig. 12a) excavation will cause serious damage to the surrounding rock mass on both the sidewalls with local failure zones, which influences the uniformity of TBM grippers' support forces on the main tunnel surface, as well as the stability of TBM operations. To avoid this problem, the authors, contractors, and owners made a series of top pilot tunnel

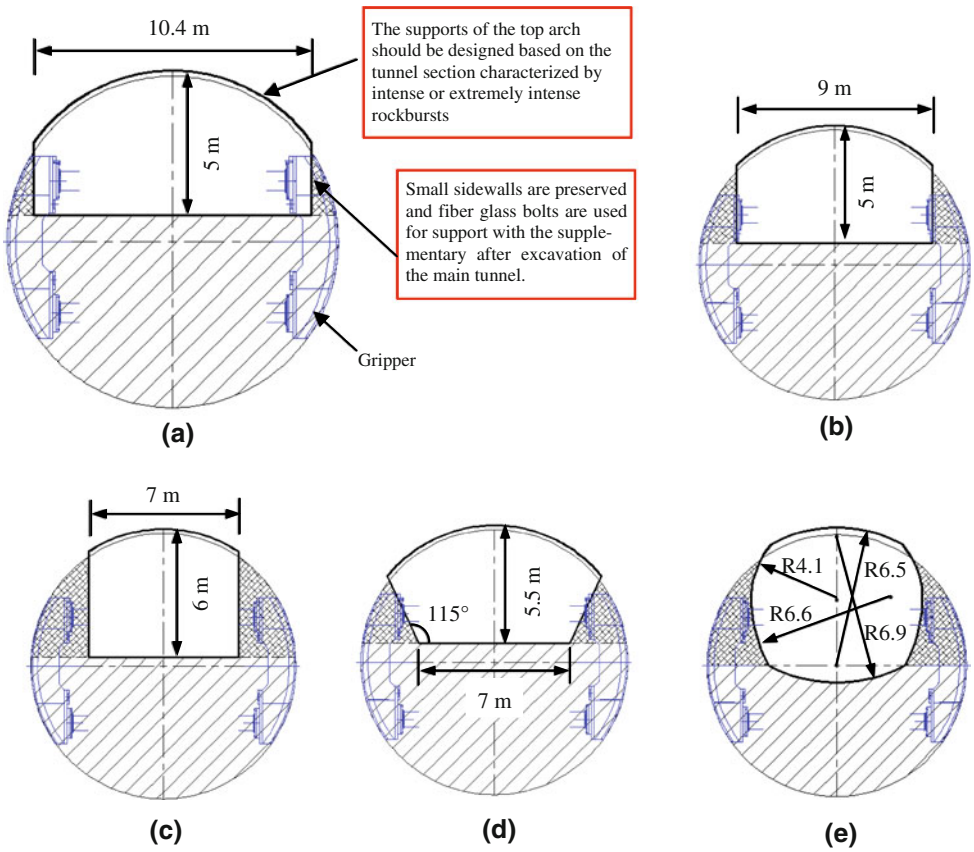

Fig. 16 The schemes for the top pilot tunnel with the small sidewalls: **a** #4; **b** #5; **c** #6; **d** #7; **e** #8

schemes for preserving small sidewalls with a specific thickness, as shown in Fig. 16a–e.

Only shotcrete and fiber glass bolts can be used for supporting the small sidewalls of the pilot tunnel and systematic supports have to be supplemented during the main tunnel excavation. Due to the different thicknesses and shapes of the small sidewalls, these schemes have different effects on the prevention of rockbursts. Obviously, the greater the thickness of the small sidewall, the worse the effect of the pilot tunnel, which may even be significantly different from the top pilot tunnel scheme, as shown in Fig. 12a. Therefore, it is necessary to conduct an independent assessment of this issue.

All of the excavation schemes analyzed are numbered in Table 3.

4.2 Assessment of the Ability to Control Strainburst

Strainbursts widely occurred in the headrace tunnels #2 and #4. For example, a series of intense strainbursts occurred from the north sidewall to the spandrel of the tunnel section K11+027-11+046 with a depth of 1,900 m in the headrace tunnel #2, as shown in Fig. 17a, where the failure zone had a depth up to 2 m. The tunnel profile after the rockburst is shown in Fig. 17b. Extremely intense strainbursts occurred from the south arch foot to the sidewall of the tunnel section K9+728-9+795 with a depth of 2,340 m and a maximum failure depth of 5 m in the headrace tunnel #4, causing a drilling machine to be smashed, as shown in Fig. 18.

Because the headrace tunnels #1 and #3 are parallel to these two tunnels with a spacing of 60 m under approximately equal in situ stress and geological conditions, the intense strainbursts are anticipated during TBM excavation. Therefore, it is necessary to assess the ability of the various schemes to handle strainbursts (Table 3).

Although the classification of rockburst intensity has been established for the headrace tunnels, the correspondence between various grades of intensity and the ERR has not been confirmed. Due to different engineering properties and scales, the empirical relationship obtained in mining engineering cannot be applied to this project directly. However, a referential ERR value is necessary for the rational evaluation, which corresponds to the most intense strainburst which can be controlled by the feasible support measures.

Table 3 Serial numbers of the various pilot schemes

Scheme	Serial no.
Full-face excavation	#1
Fig. 12b	#2
Fig. 12a	#3
Fig. 16a	#4
Fig. 16b	#5
Fig. 16c	#6
Fig. 16d	#7
Fig. 16e	#8

Based on the analysis of support responses and damage characteristics of the intense rockbursts in the headrace tunnel #2 (Fig. 17), initial supports for rockburst prevention did not meet the design requirements. According to the on-site assessment by engineers, the designed support measures can resist such levels of rockburst and hold the fractured rock masses in spite of the inevitable damage to them. Therefore, the rockbursts shown in Fig. 17 can be considered as a controllable case, and the event with a greater intensity will exceed this controllable one.

Therefore, a back-analysis is conducted on the intense rockburst in the headrace tunnel #2. The calculated ERR is adopted as a reference value to assess the advantages and disadvantages of each scheme. The ERR value of the headrace tunnel #2 after the upper bench excavation is calculated as 0.20 MJ/m^3. Figure 19 shows the values of the ERR for each scheme in Table 3 at a 2,500-m depth after the excavation of the pilot and main tunnels. Note that an ERR of 0.24 MJ/m^3 for the full-face TBM excavation is higher than that for the headrace tunnel #2 after the upper bench excavation, indicating that more intense rockbursts may occur in the full-face TBM excavation than in the upper bench excavation of the headrace tunnel #2. Therefore, it is further proven that pilot tunnel pretreatment is, indeed, necessary.

Figure 19a shows that, in both the central pilot tunnel and top pilot tunnel schemes, except for Scheme #3, the ERR values for the pilot tunnel excavation are lower than that for the headrace tunnel #2 and the full-face TBM excavation. In all of the pilot tunnel schemes, the ERR value for Scheme #3 (Fig. 12a) is the maximum. It is determined by the relationship between the shape of the pilot tunnel cross-section and the direction of the minimum principal stress in the in situ stress field, which is approximately vertical. Moreover, the tunnel section is an ellipse, with the long axis approximately horizontal. Thus, the vertical resilience after excavation is very high, so as to obtain the maximum ERR.

The ERR value is the minimum in Scheme #8, with a good tunnel shape. Based upon the relationship between the brittle failure locations and in situ stress direction, the vertical principal stress causes damage to both sidewalls. If the tunnel has an elliptical section with the long axis parallel to the vertical principal stress, and the long- to short-axis ratio is matched with the ratio of the principal stress magnitudes (Read 2004), the damage to the sidewalls caused by high stress can be minimized. As a particular

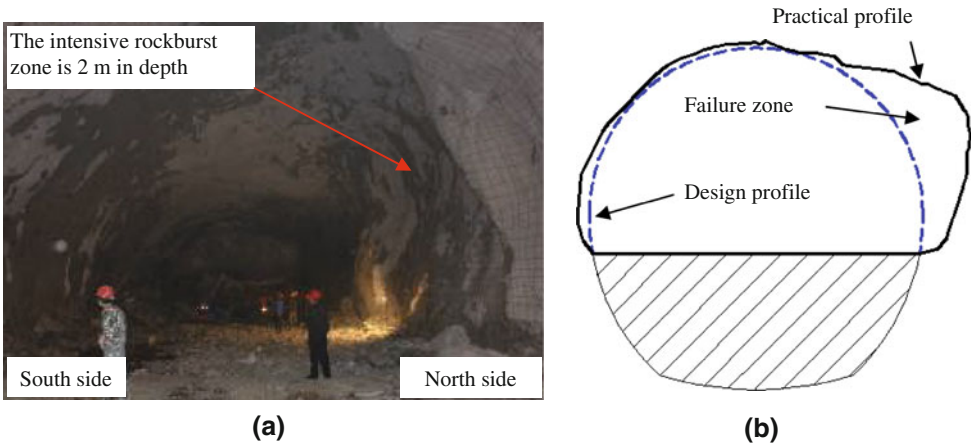

Fig. 17 The intensive rockburst from the north sidewall to the spandrel of the headrace tunnel #2: **a** the scene photo; **b** the sectional profile

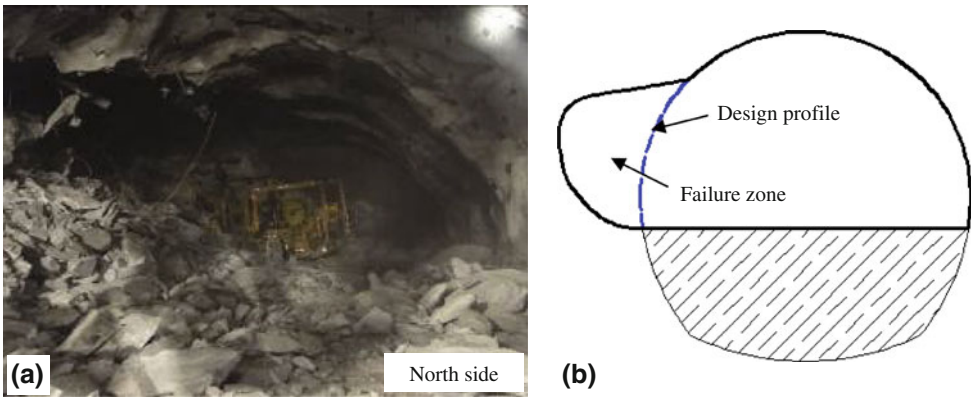

Fig. 18 The extremely intense rockburst from the south arch foot to the sidewall of the headrace tunnel #4: **a** the scene photo; **b** the sectional profile

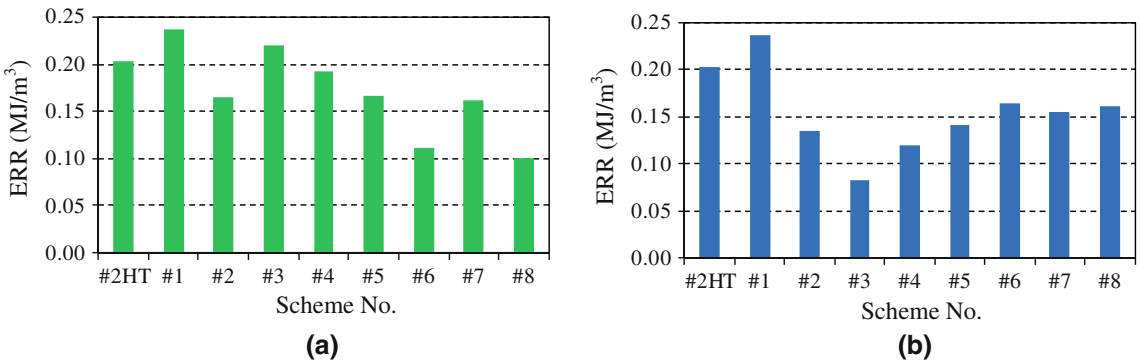

Fig. 19 The energy release rate (ERR) values of various schemes at a 2,500-m depth: **a** after excavation of the pilot tunnels; **b** after excavation of the main tunnels

failure mode, rockbursts may not follow such a law. Although the long axis of Scheme #3 is horizontal, the arch foots with the special geometry on both sides will have certain constraints on the deformation of the surrounding rock mass. This is related to the scale effect that can cause the V-shaped failure to stop at a certain depth (Martin 1993, 1997). The above analysis indicates that, although the ERR value for Scheme #3 is high, it may not mean a higher risk for rockbursts. The comparison of the ERR values in Fig. 19a between the pilot tunnel schemes and the headrace tunnel #2 indicates that the risk of an intense or extremely intense rockburst may drop during the pilot tunnel excavation.

In Fig. 19b, the ERR values in the main tunnel excavation for all pilot tunnel schemes at a 2,500-m depth are lower than the reference value, indicating that the pilot tunnel excavation can, indeed, reduce the intensity of rockbursts. Figure 19b also shows that the ERR values in the main tunnel excavation of Schemes #3 and #4 are significantly lower than that in the main

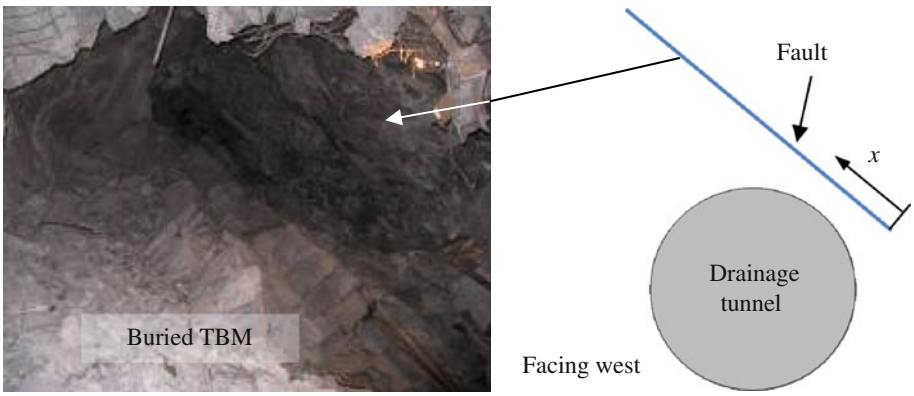

Fig. 20 The occurrence of the fault at the location of an extremely intense rockburst, called the "11.28" event, in the drainage tunnel

tunnel excavation of Scheme #2. The ERR value for Scheme #5 is nearly equal to that of Scheme #2, but the values of the other top pilot tunnel schemes are slightly higher than the latter. It indicates that the top pilot tunnel schemes can better reduce the intensity and even the frequency of intense rockbursts than the central pilot tunnel scheme. But with the thickness of the reserved small sidewalls increasing, as well as the sectional shape and size approaching those in the central pilot tunnel scheme, this advantage gradually disappears. In fact, the sidewall thickness in Schemes #4 and #5 can completely meet the support scope requirements of the grippers.

4.3 Assessment of the Ability to Control Fault-Slip Rockbursts

Geological discontinuities (joint, fault, or dyke contact) and their interaction with in situ stresses and excavation-induced stresses are very important in controlling the failure mode and intensity of the rock mass. Under the conditions of high stress, the strike and dip angle of the discontinuities with a particular relationship to the tunnel surface may induce a fault-slip rockburst.

Although the fault-slip rockbursts do not develop as widely as the strainbursts in the headrace tunnels, the resulting damages are very serious. The extremely intense rockburst in the drainage tunnel, as shown in Fig. 9d, was induced by a rigid fault near the tunnel roof, with the strike approximately parallel to the tunnel axis, a NNE dip direction, and a dip angle of 40–50°, as shown in Fig. 20. The TBM equipment was destroyed in this rockburst. Due to the major damage caused by this type of rockburst, it cannot be permitted during TBM excavation. Therefore, it is necessary to assess the abilities of all pilot tunnel schemes to prevent the fault-slip rockbursts. The shear failure along a discontinuity is the only concern in this study, rather than the magnitude of the induced seismic event.

In order to prevent a fault-slip rockburst during TBM excavation, the following measures should be adopted: (1) to encourage pre-existing fractures to slip (Toper et al. 2000) or induce a fault-slip rockburst in advance; (2) to change the conditions under which a fault-slip rockburst may occur and to control when it would occur; (3) to adopt reinforcement steps so that no slips in any position of the structural plane take place during the main tunnel excavation.

Before the outbreak of a fault-slip rockburst, the presence of the discontinuities is difficult to predict. Therefore, considering that the most threatening rockburst of this type for the TBM equipment and personnel occurs when a fault is located above the tunnel crown, the extremely intense rockburst shown in Fig. 9d is taken as a case study for the headrace tunnels. The strike and dip angle of the fault shown in Fig. 20 are estimated, and its static cohesion and friction angle are obtained by the back-analysis based on the ESS method.

Figure 21 shows the shear stress $|\tau|$ and static shear strength τ_s of the fault shown in Fig. 20. Note that the shear stress along the fault with $x = 4.5$ m is greater than the static shear strength, indicating the initiation of shear slip.

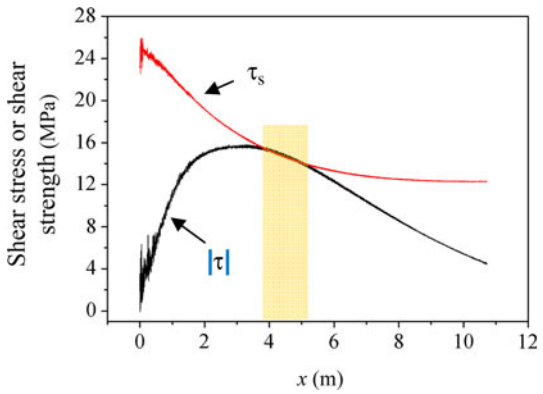

Fig. 21 The curves for the shear stress and static shear strength along the fault in the drainage tunnel

However, the shear stresses and static shear strengths in the various schemes calculated indicate that the pilot tunnel excavation may not induce a slip along the fault. Thus, the minimum difference between the static shear strength and shear stress along the fault is used for comparing the advantages and disadvantages of various schemes.

The values of $\tau'_{\min}$ along the fault in the various schemes after the pilot tunnel excavation are shown in Fig. 22. Note that the $\tau'_{\min}$ value in the central pilot tunnel scheme is somewhat higher than that computed for each top pilot tunnel scheme. This value is determined by the spatial relationship of the central pilot tunnel, main tunnel, and fault on the crown. Due to a very slight disturbance of the fault induced by the central pilot tunnel excavation, it is difficult to induce its sliding, and may even lead to the fault being ignored. As a result, such a fault may cause an intense rockburst during the main tunnel excavation. It is difficult to meet the requirement of preventing a fault-slip rockburst.

The central pilot tunnel scheme is easier to survey and to treat a fault at the bottom arch of the tunnel than the top pilot tunnel scheme. Based on practical experience during the previous upper–lower bench excavation of the headrace tunnels #2 and #4 with the D&B method, a fault-slip rockburst never occurs at the bottom arch during the lower bench excavation.

Among the top pilot tunnel schemes, Schemes #3 and #4 have the best effect with a minimum thickness for the reserved sidewalls and a large excavation size, leading to a large disturbance on the stress field in the surrounding rock mass of the main tunnel. This is likely to cause a slip along the fault. Schemes #6 and #8 with a maximum thickness of preserved sidewalls have the worst effect. Even so, pretreating with the destress blasting method in these schemes is less difficult than in the central pilot tunnel scheme.

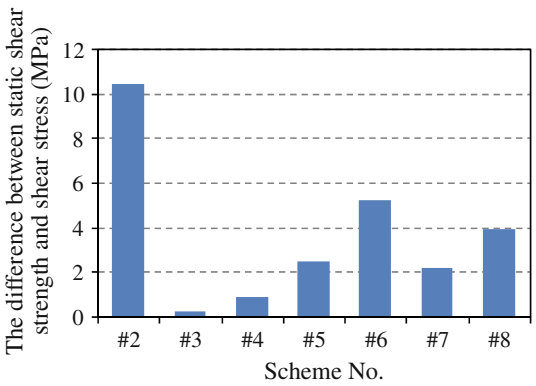

Fig. 22 The minimum difference between the static shear strength and shear stress along the fault of various pilot schemes in the pilot excavation

In summary, the top pilot tunnel method is superior to the central pilot tunnel method in its ability to control a fault-slip rockburst.

4.4 Overall Comparison

Combining the results of the above analysis, the following remarks are made:

1. The top pilot tunnel method can maximize the disturbance in the upper half of the rock mass around the main tunnel, resulting in damage as well as high stress transfer. At the same time, the main tunnel excavation has little influence on the upper part, so as to minimize the risk for rockbursts. But, a stress transfer will take place to the excavation boundary of the main tunnel after the central pilot tunnel excavation, which may increase the risk for rockbursts during TBM excavation.
2. According to the ERR results, the excavation of the top pilot and central pilot tunnels can reduce the intensity of strainburst, and even its frequency. However, the schemes with smaller preserved sidewalls are to be preferred to the central pilot tunnel scheme. Although the prevention effect can be enhanced by increasing the size of the central pilot tunnel, no advantage exists compared with full-face D&B excavation.
3. According to the ESS results, the top pilot tunnel method is more effective in preventing a fault-slip rockburst than the central pilot tunnel method with the preserved sidewalls as small as possible.

In addition to the above mechanical analysis, construction feasibility is the other important issue that should be included in the comprehensive assessment. In construction, the top pilot tunnel method has the following advantages:

1. During the top pilot tunnel excavation, the crown of the main tunnel is completely exposed. All of the possible prevention measures, such as support and destress blasting, can be chosen in order to reduce the risks of rockbursts.
2. The excavation section is large, as is the space for the operation of construction equipment, leading to improved construction efficiency.
3. The schemes are flexible and have high adaptability.

Its disadvantage is that an uneven upper–lower loading on the cutter head during TBM excavation will influence the safety of the main beam. It may be necessary to adjust the TBM excavation parameters to accommodate the half-section excavation. In addition, the rock mass at the pilot tunnel boundary may cause damage to the TBM cutters and reduce their service lives. In fact, the rock masses surrounding the pilot tunnel are fractured under high stress;

Table 4 Comparison of the advantages and disadvantages of the pilot schemes

Top pilot method	Central pilot method
Advantages	
1. The excavation section is larger, and a greater number of structural planes are exposed in the same rock mass structure, leading to a change of energy dissipation and failure mode of the rock mass	1. There is no special requirement for the TBM excavation parameters due to the symmetrical shape of the tunnel face
2. The greater disturbance and stress transfer are caused after excavation of the upper half section, effectively reducing the threat from the upper half-section during the main tunnel excavation and is beneficial to energy release in the lower part section	2. The destress blasting and other methods can be flexibly used for preventing rockbursts during the pilot tunnel excavation
3. It is beneficial to reduce strainbursts and fault-slip rockbursts during TBM excavation	3. Fiber glass bolts and shotcrete can be applied for temporary support
4. Destress blasting and other methods can be flexibly used for preventing rockbursts during the pilot and main tunnel excavations	
5. The exposed section of the main tunnel can be directly supported to ensure the stability of the rock mass on the crown during TBM excavation	
6. The pilot tunnel size is convenient for equipment operation, improving construction efficiency	
7. The scheme is flexible, with strong adaptability	
Disadvantages	
1. An uneven upper–lower loading exists on the cutter head during excavation, which may have a certain influence on the main beam. The adjustment of TBM excavation parameters may be required for the situation of half-section excavation	1. The central pilot is shaped like a gate, equivalent to the size of the auxiliary and drainage tunnels. A great risk for rockbursts exists in the pilot excavation
2. The rock mass at the pilot profile may cause damage to the TBM cutters and reduce their service life	2. After the central pilot excavation, high energy is concentrated adjacent to the excavation boundary of the main tunnel. The risk of intense rockbursts may increase during TBM excavation
	3. The pilot tunnel size is small and detrimental to equipment operation, reducing operation efficiency
	4. An increase in the pilot size may directly cause the selection of the full-face excavation scheme using the D&B method
	5. The strength of the supports consisting of shotcrete and fiber glass bolts is so low that they cannot effectively resist the impact of rockburst, especially during the main tunnel excavation
	6. The prevention capacity of the fault-slip rockburst is poor, which may even lead to the controlled structural plane being ignored

their rigidity and strength are significantly lower than those of the intact rock masses.

The advantage of the central pilot tunnel method is that there is no special requirement for the TBM excavation parameters due to the symmetrical shape of the tunnel face. However, the strength of the supports consisting of shotcrete and fiber glass bolts is so weak that they cannot effectively resist the impact of rockburst, especially during the main tunnel excavation.

No matter which kind of pilot tunnel scheme is selected, the pilot tunnel can be used as a rescue channel after an intense or extremely intense rockburst occurs during TBM excavation.

A comprehensive comparison of both methods is shown in Table 4. The top pilot tunnel method is recommended based on its reasonable mechanics and construction feasibility.

5 Evaluation of Application Effect and Practice

5.1 On-Site Experiment of the Top Pilot Tunnel Method

After an intense rockburst occurred in the headrace tunnel #2 (Fig. 17), given the approximately equal in situ stress and geological conditions in the parallel headrace tunnel #3, an intense or extremely intense rockburst is expected. To verify the effect of the top pilot tunnel method on preventing rockbursts, taking into account the safety of the TBM cutter head and main beam, Scheme #8 was used. The experimental pilot tunnel section has the number K11+181-11+131 with a length of 50 m. The support design parameters are shown in Fig. 23 (Zhou 2011). After the pilot tunnel excavation, a 10-cm-thick CF30 nano steel fiber-like concrete was first sprayed at the crown and

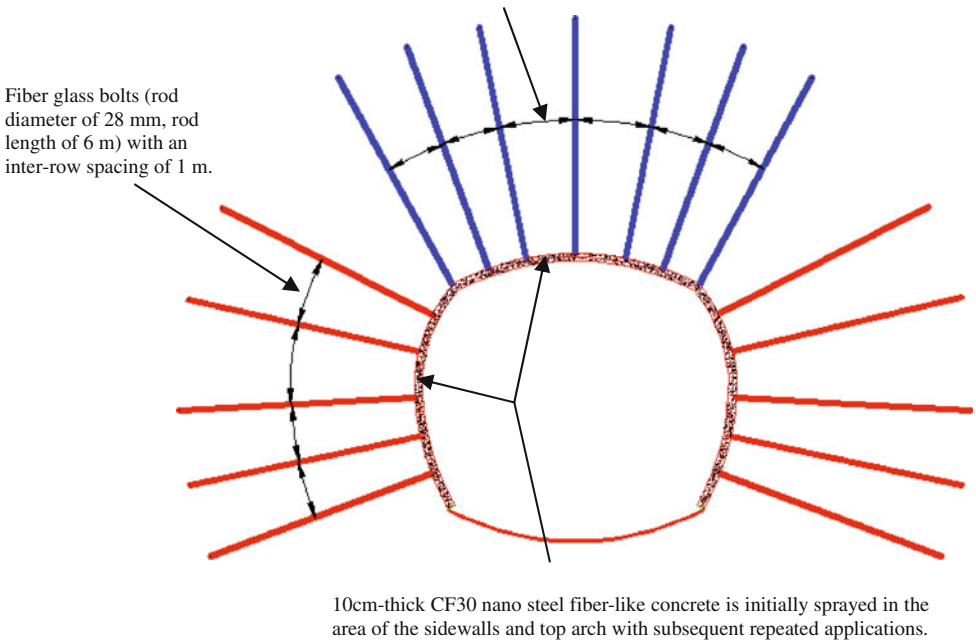

Fig. 23 The support measures of the top pilot tunnel in the experimental section of the headrace tunnel #3 (Zhou 2011)

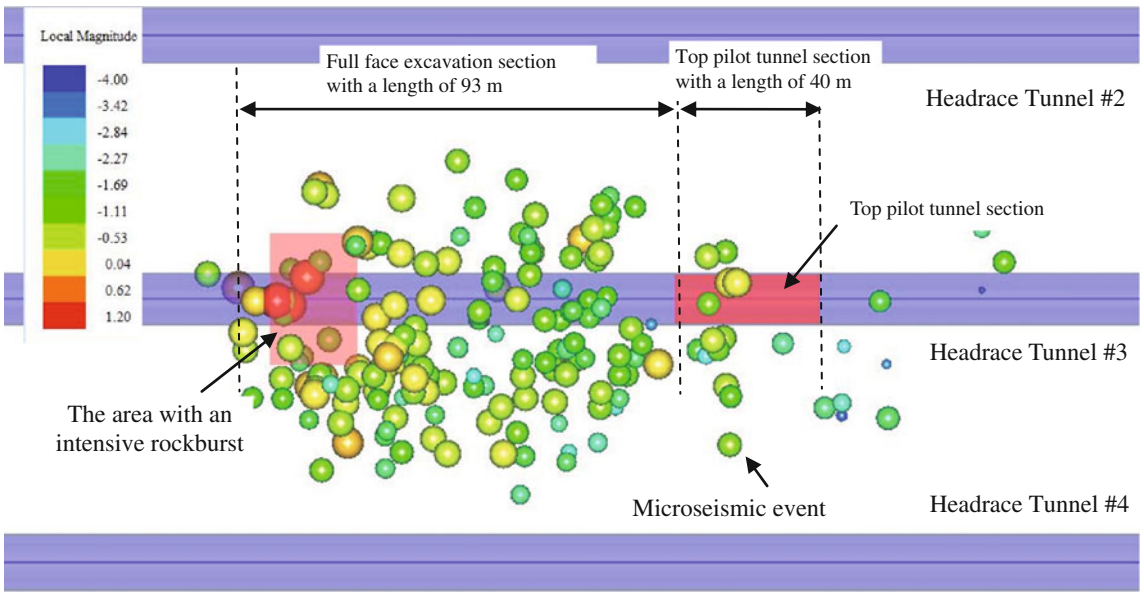

Fig. 24 The distribution of events obtained through microseismic monitoring in the experimental top pilot tunnel section in the headrace tunnel #3

sidewalls, and expansion shell-anchored rock bolts (rod diameter of 32 mm, rod length of 6 m) were installed with an inter-row spacing of 1 m and a top-arch bolt plate size (length × width × thickness) of 400 mm × 400 mm × 10 mm. Fiber glass bolts (rod diameter of 28 mm, rod length of 6 m) were installed with an inter-row spacing of 1 m and no plates were installed at the sidewalls. These supports provided a safe operating environment during excavation with the D&B method.

Although this tunnel section was prone to intense or extremely intense rockbursts, such occurrence could not be confirmed. Thus, it was difficult to assess the effect of the top pilot tunnel method on reducing the risk of rockbursts. The microseismic monitoring method was applied in the

Fig. 25 The layered fracture in the surrounding rock mass of the headrace tunnel #3 during the full-face TBM excavation (Zhang et al. 2011b)

TBM excavation (Xiao et al. 2011). Moreover, the monitoring range was extended to a specific full-face excavation section, as shown in Fig. 24, in order to better compare the responses of the surrounding rock mass during TBM excavation with the presence of the top pilot tunnel and without it.

As shown in Fig. 24, the section with the top pilot tunnel excavated in advance had a small number of microseismic events during the TBM excavation. Thus, the conclusion of Sect. 4.1 was confirmed, i.e., the main tunnel excavation by TBM has little influence on the upper half of the section, as no rockbursts occurred. In the contrary, when the TBM entered the full-face excavation section, the microseismic events increased and intensified significantly, and severe layered fractures were created in the surrounding rock mass, as shown in Fig. 25 (Zhang et al. 2011b). Additionally, several light- to middle-class rockbursts occurred.

The above microseismic monitoring results and the responses of the surrounding rock mass in the sections with and without the pilot tunnel indicate that the top pilot tunnel method is very effective in reducing the intensity and frequency of rockbursts during TBM excavation. Moreover, based on the on-site assessment, it was concluded that the pilot tunnel has an insignificant influence on the main beam and cutter head of the TBM and cause no damage to the equipment.

5.2 Application of the Top Pilot Tunnel Method in Production

The top pilot tunnel method was utilized for several sections prone to intense or extremely intense rockbursts in the headrace tunnels #1 and #3.

In the section K11+061-10+867 of the headrace tunnel #1, Scheme #5 was chosen. The support measures of the pilot tunnel are shown in Fig. 26. No rockburst occurred during the excavation of the top pilot and main tunnels, with only slight spalling and fracturing. The TBM successfully passed this section.

Scheme #4 was applied in the extremely intense rockburst section of the headrace tunnel #3, which has the same geological and in situ stress conditions as the sections of the drainage tunnel shown in Fig. 9d and the headrace tunnel #4 shown in Fig. 18. The support measures of the pilot tunnel are the same as those shown in Fig. 23. Figure 27 shows the on-site excavation and support of the top pilot tunnel.

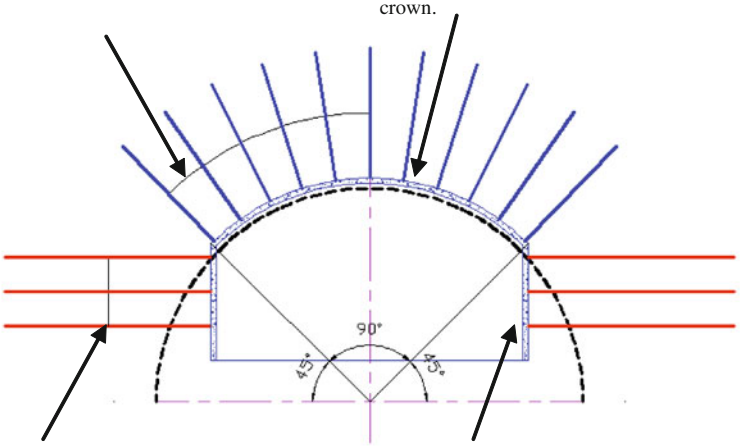

Fig. 26 The support measures for the top pilot tunnel in the section K11+061-10+867 of the headrace tunnel #1

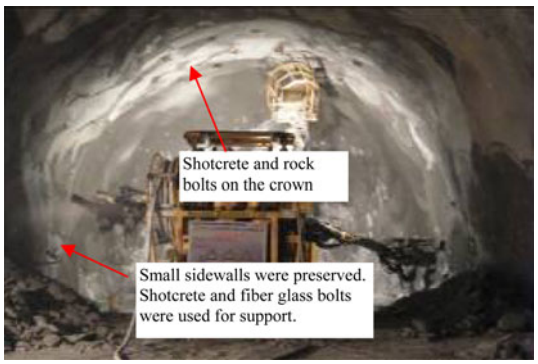

Fig. 27 Photo of the excavation and support of the pilot tunnel in the headrace tunnel #3

Fig. 28 The collapse of the fractured rock mass on the south sidewall of the headrace tunnel #3 during the TBM excavation

Due to the very high stress level, a large number of collapses of the fractured rock mass on both sidewalls during the TBM excavation occurred, as shown in Fig. 28. These indicate that the mechanical properties and failure modes of the rock mass were changed by the pilot tunnel excavation. Although the advance speed of the TBM was slowed down by the sidewall collapses, no rockbursts occurred. The surrounding rock masses supported on the top arch maintained good stability, providing a safe environment for the support operation in the L1 area.

When the TBM successfully passed the pilot tunnel section, no extremely intense rockbursts were anticipated at the next section without the pilot tunnel. Unfortunately, the TBM drove forward only 60 m and was shut down by an intense rockburst at the north sidewall at K9+655. The failure zone had a depth of 3.5 m, as shown in Fig. 29. It indicated that the extremely intense rockburst section was not passed.

The above practices of the top pilot tunnel indicate that this method is very effective at preventing rockbursts during TBM excavation.

Fig. 29 The intensive rockburst on the north sidewall of the headrace tunnel #3 during the full-face TBM excavation

6 Conclusions

Based on the engineering practices in the drainage tunnel and the headrace tunnels at the Jinping II Hydropower Station, it has been shown that the tunnel boring machine (TBM) equipment has a low capacity to resist the impact of a rockburst. The traditional full-face TBM excavation method cannot handle the intense or extremely intense rockbursts in deep hard rock tunnels, which easily results in equipment damage and casualties. With the aim to solve this problem, the excavation and support pretreatments with the top pilot tunnel drilling and blasting (D&B) method have firstly been proposed in this study. Then, its effect on rockburst prevention is discussed from both theoretical and construction points of view. Finally, this method is applied in several intense or extremely intense rockburst sections in the headrace tunnels #1 and #3. Based on the above analysis and application results, the following conclusions can be drawn:

1. The top pilot tunnel excavation can maximize the disturbance in the rock mass surrounding the upper half section of the main tunnel and change its mechanical properties and failure modes, leading to a stress transfer and a reduction in the risk of rockbursts during the TBM excavation. On the contrary, the central pilot tunnel method may cause enhancement of the intensity and frequency of rockbursts.
2. From the perspective of controlling strainbursts and fault-slip rockbursts, the top pilot tunnel schemes with the smaller-sized reserved sidewalls have been shown to be preferable with respect to the central pilot tunnel scheme.
3. During the top pilot tunnel excavation, geophysical surveys, geological mapping, and other means can be used to understand the geological conditions and assess the risk of rockbursts. Moreover, destress blasting, support, and other measures can be flexibly applied to prevent rockbursts. The powerful supports

of the crown can effectively ensure the safety of the operating space during TBM excavation. The risk of rockbursts in the main tunnel can be assessed based on the known geological conditions. And the flexible pretreatment approaches can be applied through the pilot tunnel during TBM excavation.

4. According to the microseismic monitoring results of the field test section and the practical effects of application to the sections prone to intensive and extremely intense rockbursts, it has been proven that the top pilot tunnel method can reduce the risk of rockbursts by pretreatment. It is an effective method to handle intensive and extremely intense rockbursts in TBM excavation.

Acknowledgments The authors gratefully acknowledge the financial support from the National Science Foundation of China under Grant Nos. 2010CB732006, 51079144, and 50979104, and the National Science Foundation of Hubei Prince in China under Grant No. 2010CDB10404. The work in this paper was also supported by research funding from the Ertan Hydropower Development Company, Ltd., and an important pilot tunnel project (for youth talent) of the knowledge innovation project of the Chinese Academy of Sciences (CAS) (No. KZCX2-EW-QN115). We are also grateful for the support and assistance of the engineers at the East China Investigation and Design Institute with the headrace tunnel design and construction. Special thanks go to Prof. Giovanni Barla and the two anonymous reviewers for their constructive comments.

References

Board MP (1994) Numerical examination of mining-induced seismicity. PhD thesis, University of Minnesota, Minneapolis, MN, USA

Brady BHG, Brown ET (2006) Rock mechanics for underground mining, 3rd edn. Springer, Dordrecht, The Netherlands

Broch E, Sørheim S (1984) Experiences from the planning, construction and supporting of a road tunnel subjected to heavy rockbursting. Rock Mech Rock Eng 17:15–35

Brown ET (1984) Rockbursts: prediction and control. Tunnels Tunnell 84:17–19

Canadian Rockburst Research Program (CRRP) (1996) A comprehensive summary of five years of collaborative research on rockbursting in hard rock mines. CAMIRO Mining Division, CRRP

Cook NGW, Hoek E, Pretorius JPG, Ortlepp WD, Salamon MDG (1966) Rock mechanics applied to the study of rockbursts. J S Afr Inst Min Metall 66:435–528

Goodman RE (1980) Introduction to rock mechanics. Wiley, New York

Hajiabdolmajid V, Kaiser PK, Martin CD (2002) Modelling brittle failure of rock. Int J Rock Mech Min Sci 39:731–741

Hoek E, Kaiser PK, Bawden WF (1997) Support of underground excavations in hard rock. Taylor & Francis, New York

Li T, Cai MF, Cai M (2007) A review of mining-induced seismicity in China. Int J Rock Mech Min Sci 44:1149–1171

Martin CD (1993) The strength of massive Lac du Bonnet granite around underground openings. PhD thesis, University of Manitoba, Canada

Martin CD (1997) Seventeenth Canadian Geotechnical Colloquium: the effect of cohesion loss and stress path on brittle rock strength. Can Geotech J 34:698–725

McCreath DR, Kaiser PK (1992) Evaluation of current support practices in burst-prone ground and preliminary guidelines for Canadian hardrock mines. In: Kaiser PK, McCreath DR (eds) Rock support in mining and underground construction. Balkema, Rotterdam, The Netherlands, pp 611–619

Ortlepp WD (2001) The behaviour of tunnels at great depth under large static and dynamic pressures. Tunn Undergr Space Technol 16:41–48

Ortlepp WD, Stacey TR (1994) Rockburst mechanisms in tunnels and shafts. Tunn Undergr Space Technol 9:59–65

Read RS (2004) 20 years of excavation response studies at AECL's Underground Research Laboratory. Int J Rock Mech Min Sci 41:1251–1275

Rojat F, Labiouse V, Kaiser PK, Descoeudres F (2009) Brittle rock failure in the Steg lateral adit of the Lötschberg base tunnel. Rock Mech Rock Eng 42:341–359

Roux AJA, Leeman ER, Denkhaus HG (1957) Destressing: a means of ameliorating rockburst conditions. Part I: the concept of destressing and the results obtained from its applications. J S Afr Inst Min Metall 57:101–119

Ryder JA (1988) Excess shear stress in the assessment of geologically hazardous situations. J S Afr Inst Min Metall 88:27–39

Salamon MGD (1983) Rockburst hazard and the fight for its alleviation in South African gold mines. In: Rockbursts: prediction and control. IMM, London, pp 11–36

Salamon MGD (1984) Energy considerations in rock mechanics: fundamental results. J S Afr Inst Min Metall 84:233–246

Shan Z, Yan P (2010) Management of rock bursts during excavation of the deep tunnels in Jinping II Hydropower Station. Bull Eng Geol Environ 69:353–363

Shi HG (1995) Study of rockbursts in the left-bank headrace tunnels in Ertan Hydropower Station. Des Hydropower Station 11:35–40 (in Chinese)

Singh SP (1988) Burst energy release index. Rock Mech Rock Eng 21:149–155

Stacey TR, Ortlepp WD, Kirsten HAD (1995) Energy-absorbing capacity of reinforced shotcrete, with reference to the containment of rockburst damage. J S Afr Inst Min Metall 95:137–140

Tang BY (2000) Rockburst control using distress blasting. PhD thesis, McGill University, Montreal, Canada

Toper AZ, Kabongo KK, Stewart RD, Daehnke A (2000) The mechanism, optimization and effects of preconditioning. J S Afr Inst Min Metall 100:7–16

Wu S, Shen M, Wang J (2010) Jinping hydropower project: main technical issues on engineering geology and rock mechanics. Bull Eng Geol Environ 69:325–332

Xiao YX, Feng XT, Chen BR, Feng GL, Zhang ZT, Ming HJ (2011) Rockburst risk of tunnel boring machine part-pilot excavation in very strong rockburst section of deep hard tunnel. Rock Soil Mech 32:3111–3118 (in Chinese)

Zhang CQ, Zhou H, Feng XT (2011a) An index for estimating the stability of brittle surrounding rock mass: FAI and its engineering application. Rock Mech Rock Eng 44:401–414

Zhang C, Zhou H, Feng X, Xing L, Qiu S (2011b) Layered fractures induced by principal stress axes rotation in hard rock during tunnelling. Mater Res Innov 15:S527–S530

Zhou JF (2011) Study on rockburst mechanism, prediction and prevention of deep buried-long-large tunnels in Jinping II Hydropower Station. PhD thesis, Wuhan University, China (in Chinese)